Supplement of Atmos. Chem. Phys., 20, 11181–11199, 2020
https://doi.org/10.5194/acp-20-11181-2020-supplement

Atmospheric Chemistry and Physics
Open Access

Supplement of

Elucidating the pollution characteristics of nitrate, sulfate and ammonium in $\mathrm{PM}_{2.5}$ in Chengdu, southwest China, based on 3-year measurements

Liuwei Kong et al.

Correspondence to: Xingang Liu (liuxingang@bnu.edu.cn) and Qinwen Tan (11923345@qq.com)

QA/QC (quality assurance and control, Fig. S1-S4)

Data quality control and assurance are important components of atmospheric comprehensive observation experiments. In addition to regular inspection and calibration of the equipment through professional operation and maintenance to ensure the accuracy of experimental data, the quality control and processing of monitoring data, such as excluding outliers and data beyond the detection limit, are also important. The temporal series of monitoring data are shown in Fig. S1-S4, and the red part in the figures indicates data missing and that the overall data integrity is good. The missing rate of $PM_{2.5}$ data in Fig. S1 is 6.8%. The missing rates of NO_3^-, SO_4^{2-}, NH_4^+, OC and EC data in Fig. S2 are 18.1, 17.1, 20.7, 15.2 and 19.6%, respectively. In Fig. S3, the gaseous pollution of NO data is missing 18.2%, NH_3 is missing 11.3%, and other gases are missing 9%. The quality of meteorological data is good (Fig. S4), and the overall missing rate is 3.1% or less. On the whole, the observation data are good and do not affect the continuity of the data as a whole. The Cl^-, Na^+, K^+, Mg^{2+} and Ca^{2+} data are significantly missing, and this study only involved in the analysis of the ISORROPIA-II thermodynamic equilibrium model. To ensure that each sample data point can be input into the model completely, 618 sample input models are selected according to the data quality control to eliminate the impact of missing data to ensure that the model analysis results are effective.

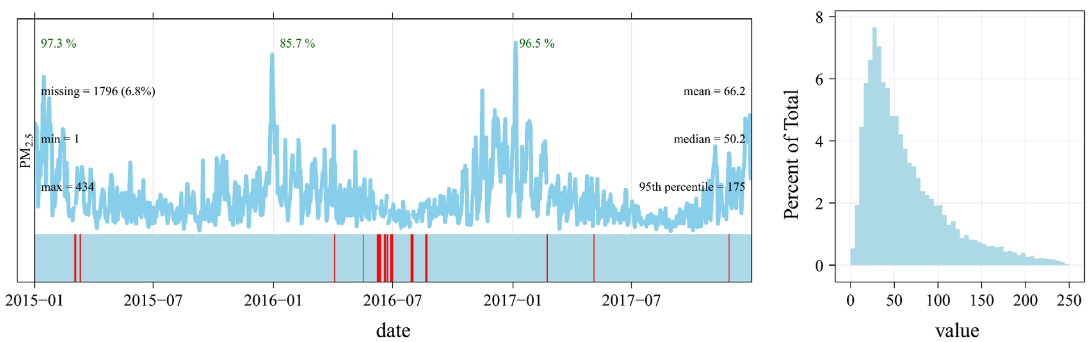

Fig. S1. $PM_{2.5}$ data quality assurance and control.

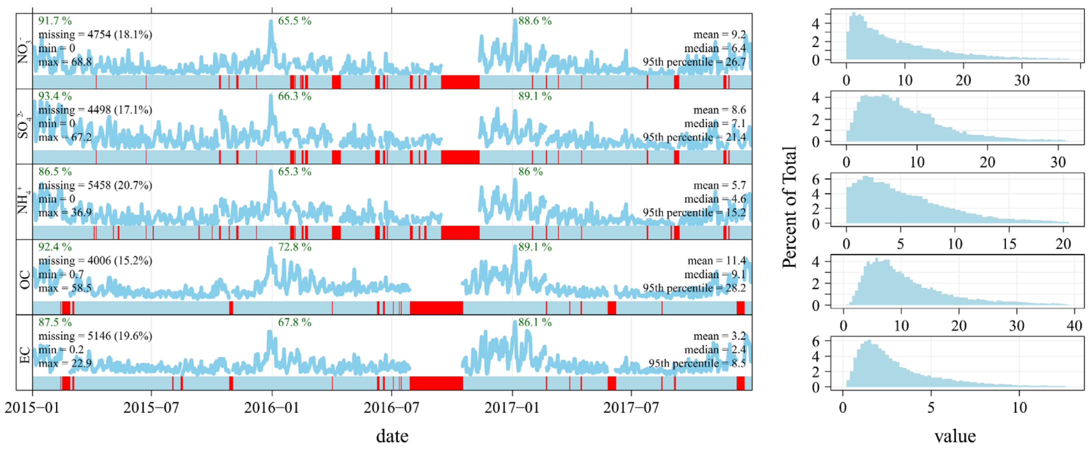

Fig. S2. NO_3^-, SO_4^{2-}, NH_4^+, OC (organic carbon) and EC (element carbon) data quality assurance and control.

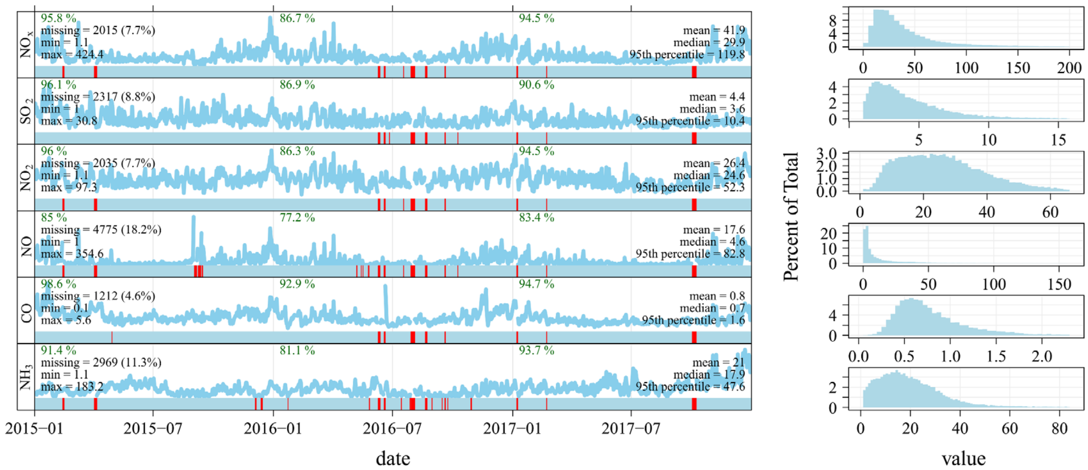

Fig. S3. NOx, SO_2, NO_2, NO, CO and NH_3 data quality assurance and control.

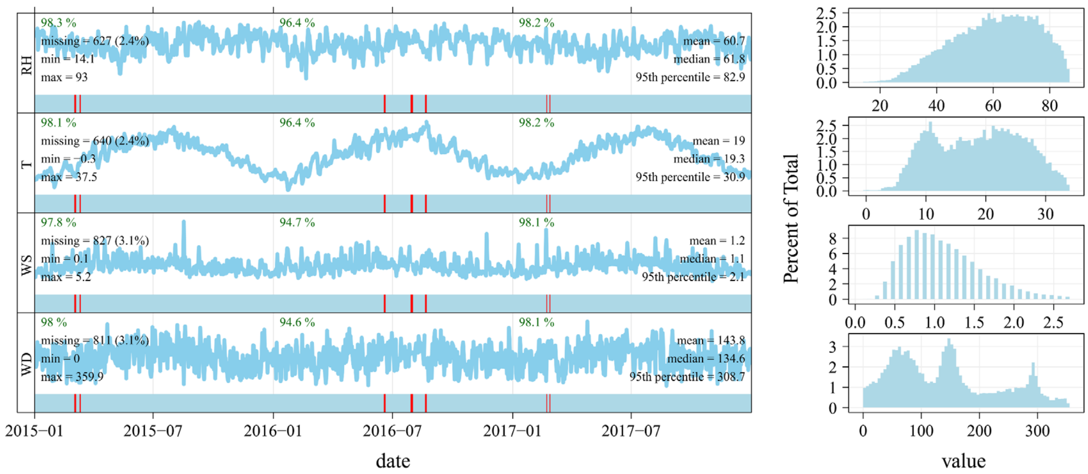

Fig. S4. Relative humidity (RH), temperature (T), wind speed (WS) and wind direction (WD) data quality assurance and control.

Table S1. Comparison of $PM_{2.5}$, NO_2 and SO_2 ($\mu g/m^3$) mass concentrations from 2013 to 2017.

	2013	2014	2015	2016	2017
$PM_{2.5}$	97	77	64	63	56
NO_2	63	59	53	54	53
SO_2	31	19	14	14	11

Data from Chengdu Municipal Ecology and Environment Bureau: Ambient air quality report, http://sthj.chengdu.gov.cn/， last access: June 17, 2020.

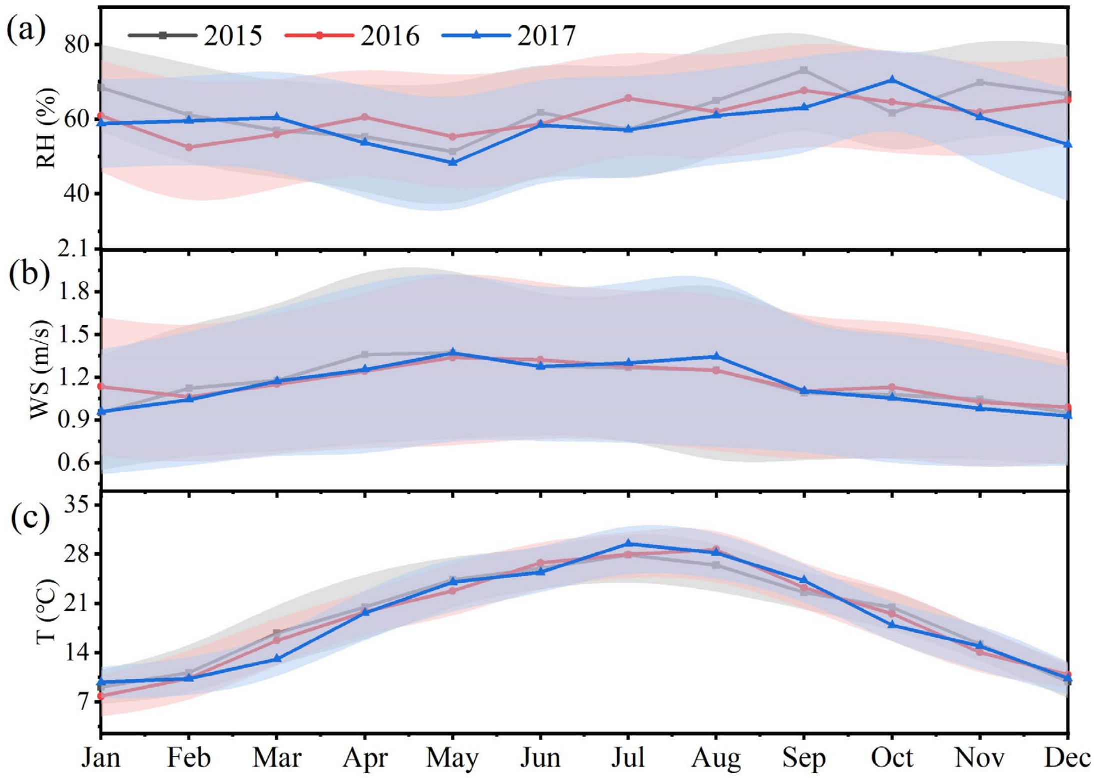

Fig. S5. Monthly variations in meteorological conditions during the observations (2015-2017). (a) Relative humidity (RH). (b) Wind speed (WS). (c) Temperature (T).

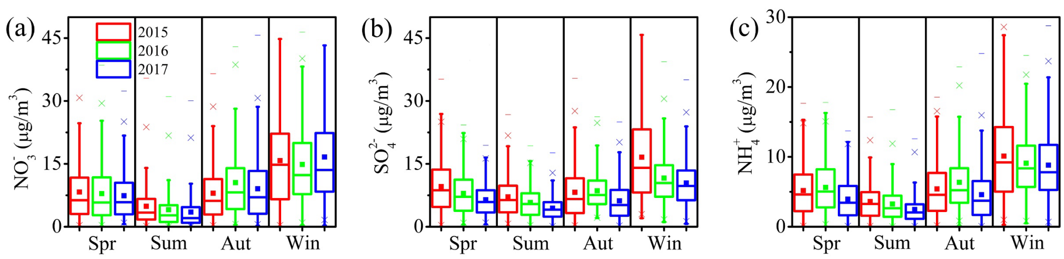

Fig. S6. Seasonal variations in NSA (nitrate, sulfate and ammonium) mass concentrations from 2015 to 2017. (a) NO_3^-. (b) SO_4^{2-}. (c) NH_4^+.

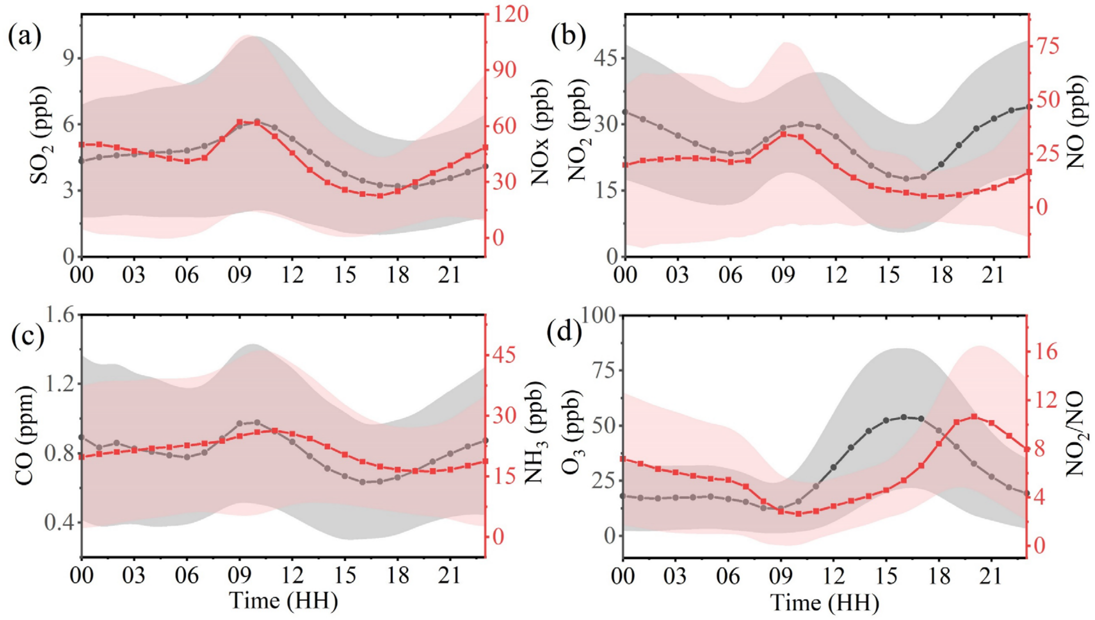

Fig. S7. Diurnal variations in gaseous pollutants from 2015 to 2017. (a) SO_2 and NOx. (b) NO_2 and NO. (c) CO and NH_3. (d) O_3 and NO_2/NO.

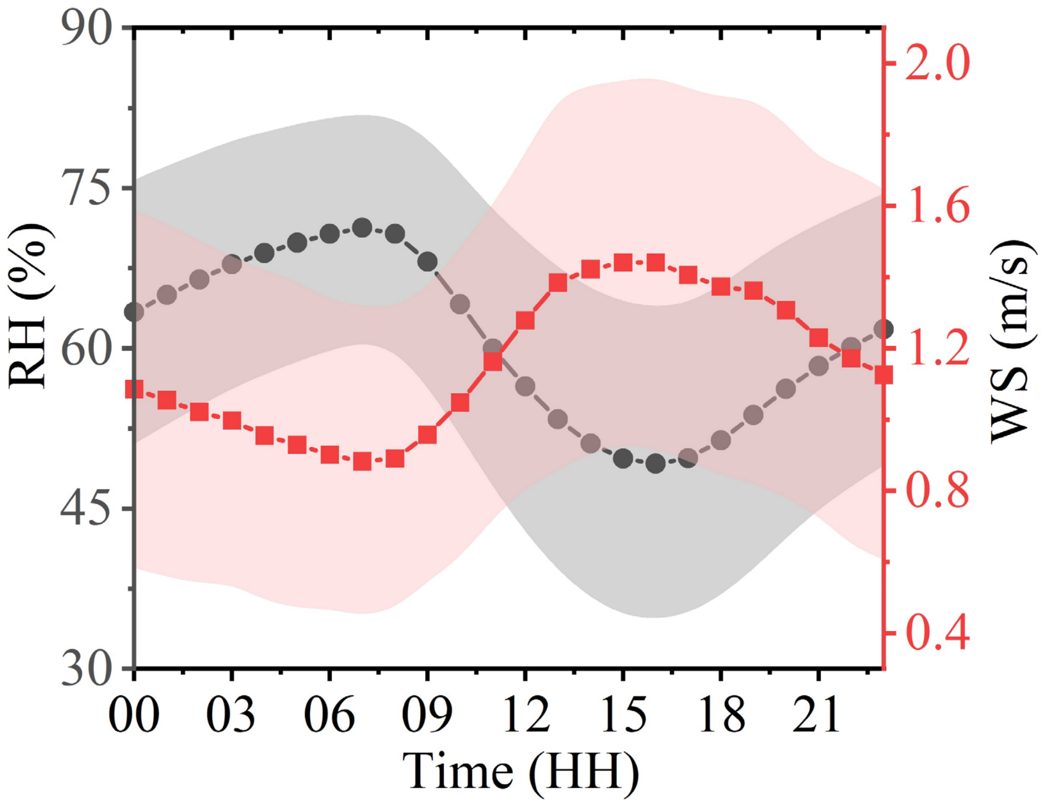

Fig. S8. Diurnal variations in metrological conditions from 2015 to 2017. Relative humidity (RH) and wind speed (WS).

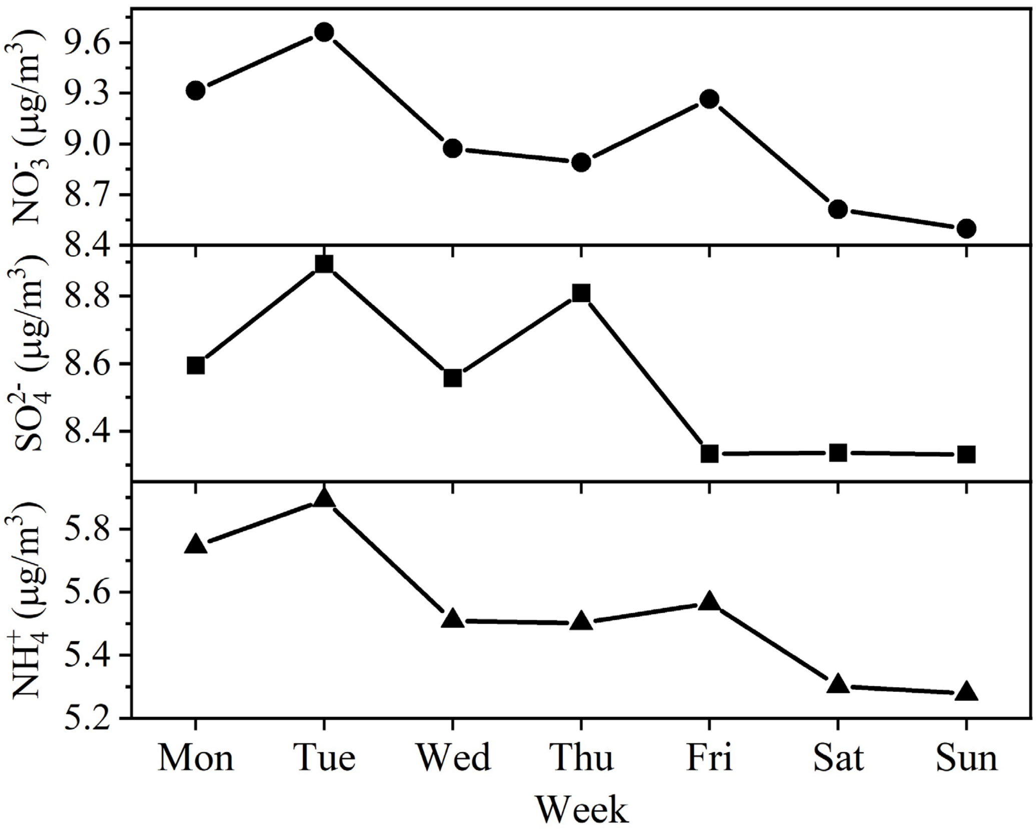

Fig. S9. Weekly variations in NSA (nitrate, sulfate and ammonium) during the overall observation period.

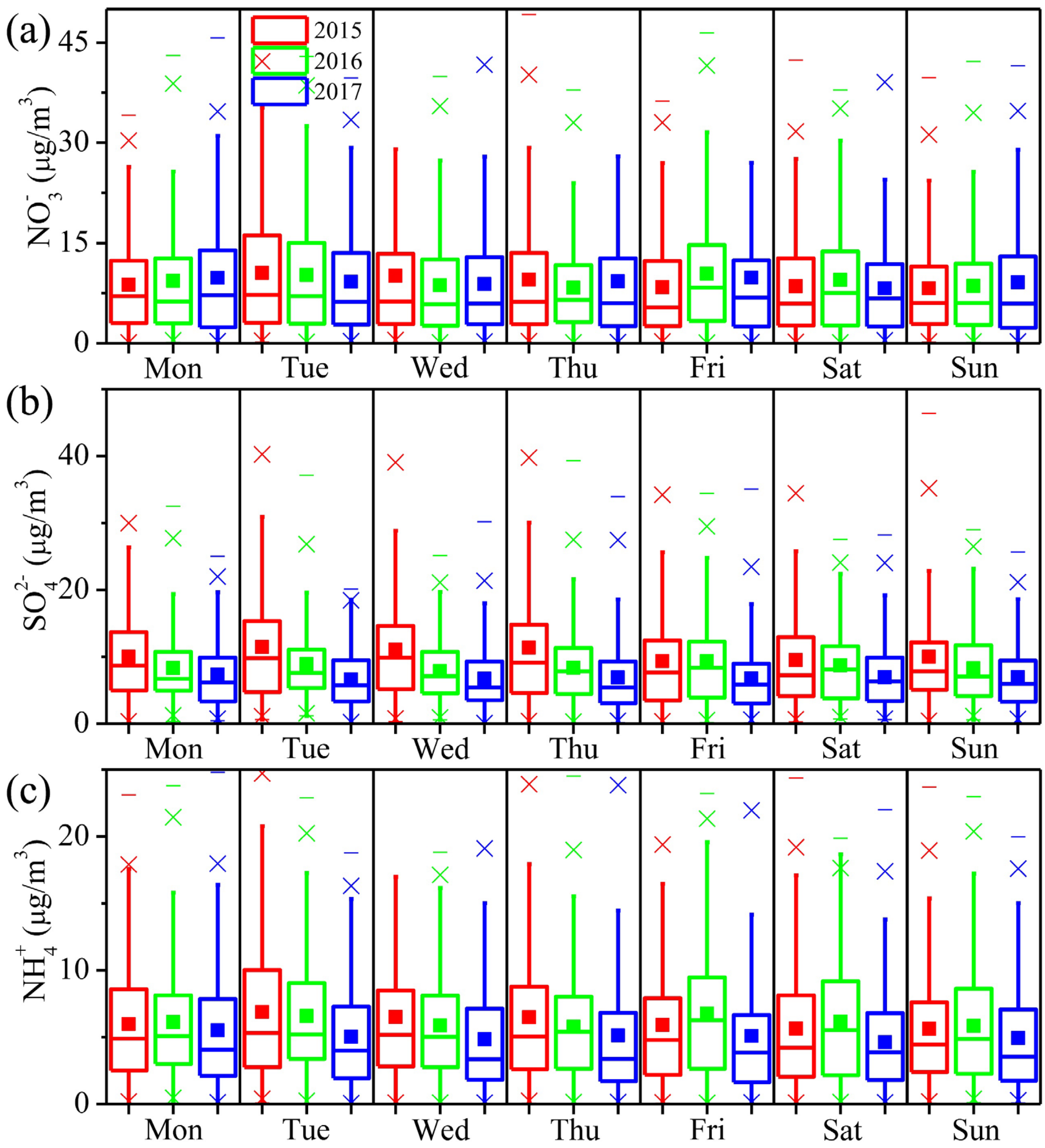

Fig. S10. Weekly variations in NSA (nitrate, sulfate and ammonium) from 2015 to 2017 (box plot). (a) NO_3^-. (b) SO_4^{2-}. (c) NH_4^+.

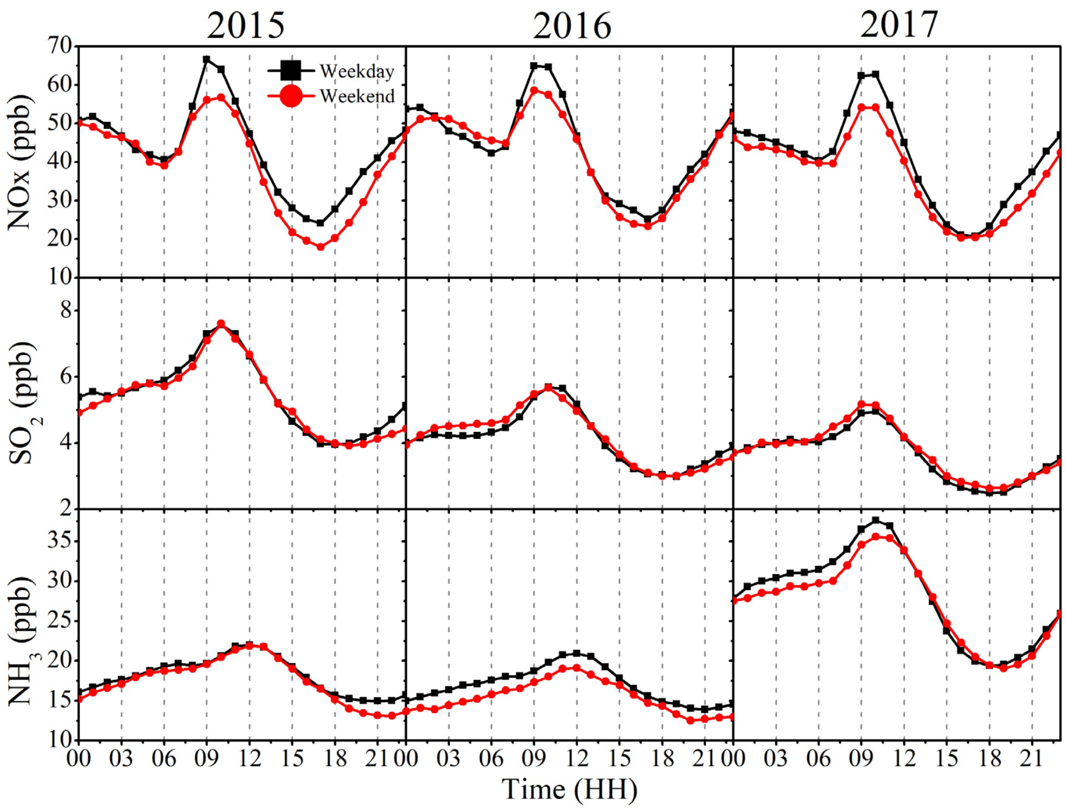

Fig. S11. Diurnal variations in NOx, SO_2 and NH_3 during weekdays (Monday to Friday) and weekends (Saturday and Sunday) from 2015 to 2017.

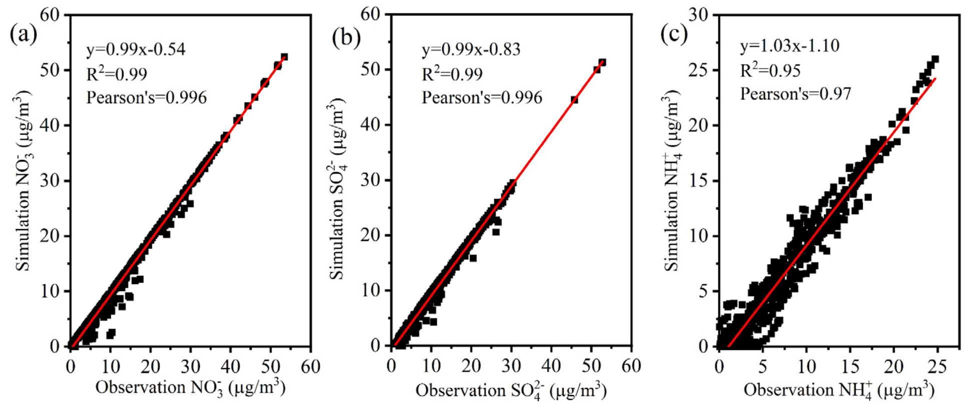

Fig. S12. The observation values of NSA (nitrate, sulfate and ammonium) are compared with the simulated values of the ISORROPIA-II thermodynamic equilibrium model. The simulated value is the NSA concentration of the liquid phase in the metastable state output by the model. (a) NO_3^-. (b) SO_4^{2-}. (c) NH_4^+.

ISORROPIA-II thermodynamic equilibrium model sensitivity analysis

The sensitivity analysis of NSA was simulated by changing the pollutant concentration input into the ISORROPIA-II thermodynamic equilibrium model by controlling the variable method. Variables: SO_4^{2-}, NO_3^- and TNH_3 (measurement data during observation periods); Invariants: temperature (T), RH, Na^+, Cl^-, Ca^{2+}, K^+ and Mg^{2+} (mean values of measurement data during observation periods). For example, to study the response of NH_4^+ and NO_3^- to changes in SO_4^{2-} concentration, the variable is SO_4^{2-}, and invariants include T, RH, Na^+, Cl^-, Ca^{2+}, K^+, Mg^{2+}, NO_3^- and TNH_3. The average value of the input data is shown in Table S2. The degree of response is expressed by the coefficient of variation: standard deviation/mean value*100.

Table S2. Input average value data of parameters of the ISORROPIA-II thermodynamic equilibrium model.

Na	SO_4^{2-}	TNH_3	NO_3^-	Cl	Ca	K	Mg	RH	TEMP
1.116	8.630	21.883	9.180	1.356	0.226	0.579	0.105	0.607	292.168

Ions units: μg/m^3; RH: relative humidity (0-1 scale); TEMP: Temperature (K); TNH_3: NH_3 + NH_4^+ (μg/m^3).

Through observation data quality control, we screened 618 sample input ISORROPIA-II thermodynamic equilibrium models to ensure the integrity of the samples and the effectiveness of the data. The control variable method was used to explore the impact of a concentration reduction for other species. For example, to explore the impact of NO_3^- concentration reduction for SO_4^{2-} and NH_4^+, the NO_3^- data were calculated based on the 5, 10, 15 and 20% emission reduction ratio, and other parameters were input into the model using the observation data to explore the relative variable of SO_4^{2-} and NH_4^+ concentration. The simulation results are shown in Table S3. When only NO_3^- and SO_4^{2-} were reduced, NH_4^+ was significantly reduced, but the changes in SO_4^{2-} and NO_3^- were not obvious, and the relative variables of approximately 12% and 7% may be mainly affected by the change in phase state. When only TNH_3 was controlled, the relative variable of SO_4^{2-} was not obvious, and the concentrations of NO_3^- and NH_4^+ decreased, but the relative variable was not large. NSA has a good reduction effect under synergistic emission reduction control. The results show that reducing the amount of NO_3^- and SO_4^{2-} can not only reduce their concentrations but also help to reduce the concentration of NH_4^+. It also suggests that controlling the gaseous precursors NOx and SO_2 is of great significance to reduce the amount of secondary inorganic aerosol in $PM_{2.5}$. Studies in Mexico City have also shown that reducing total sulfate and total nitrate rather than total ammonium helps reduce $PM_{2.5}$ concentrations in an ammonium-rich environment (Fountoukis et al., 2009).

Table S3. Simulation of NO_3^-, SO_4^{2-} and TNH_3 emission reduction control effect (%) and its influence on pH based on the ISORROPIA-II thermodynamic equilibrium model.

Reduction	Only NO_3^- Reduction				Only SO_4^{2-} Reduction			
	NO_3^-	SO_4^{2-*}	NH_4^+	pH*	NO_3^-	SO_4^{2-*}	NH_4^+	pH
5%	11.92	12.25914	8.33	4.0495	7.19	17.1088	9.77	4.08
10%	16.58	12.25911	11.13	4.0519	7.09	21.9593	13.65	4.13
15%	21.23	12.25909	13.91	4.0546	7.00	26.8093	17.50	4.19
20%	25.88	12.25906	16.69	4.0547	6.91	31.6596	21.58	4.25
	Only TNH_3 Reduction				Synergistic **			
	NO_3^-	SO_4^{2-*}	NH_4^+	pH	NO_3^-	SO_4^{2-*}	NH_4^+	pH
5%	7.51	12.25938	5.85	4.02	12.08	17.1090	12.86	4.07
10%	7.79	12.25965	6.20	3.99	16.85	21.9596	19.80	4.09
15%	8.10	12.25998	6.59	3.95	21.64	26.8097	26.17	4.11
20%	8.45	12.26040	7.03	3.91	26.37	31.6601	33.29	4.16

Notes: NO_3^-, SO_4^{2-} and TNH_3 are the concentration variables relative to the observation data; pH is the average; TNH_3: NH_3+NH_4^+ (μg/m^3);

*: In order to display the data difference, the number of digits after the decimal point was increased;

**: NO_3^-, SO_4^{2-} and TNH_3 decreased in the same proportion.

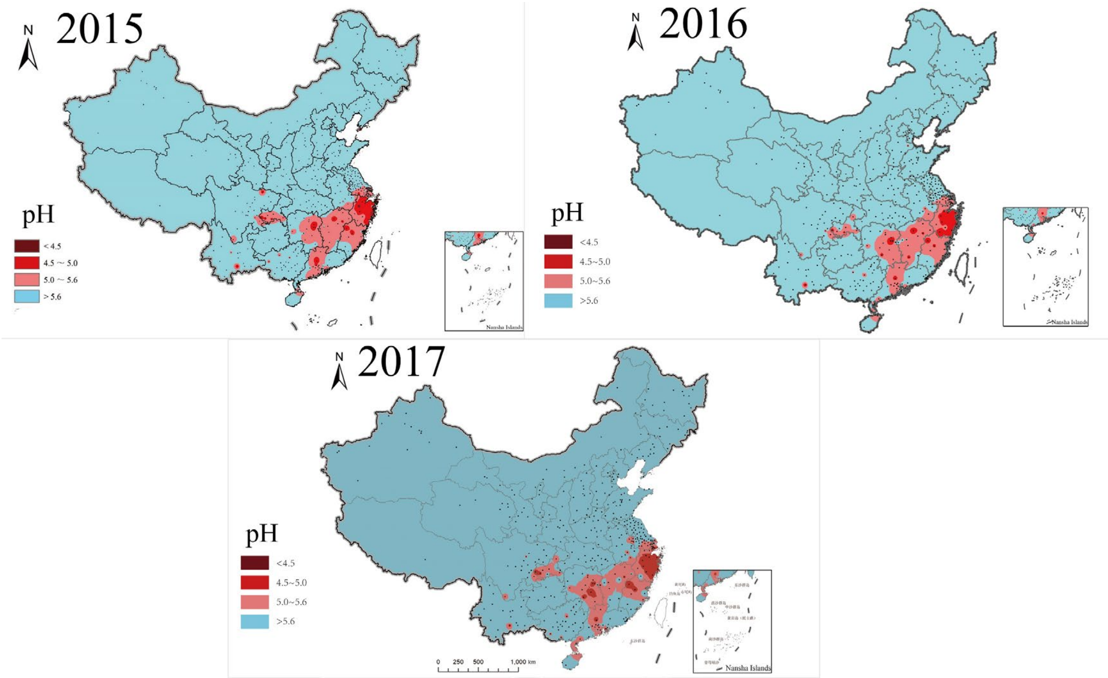

Fig. S13. Acid rain distribution in China (http://www.mee.gov.cn/hjzl/zghjzkgb/lnzghjzkgb/, last access: June 17, 2020).

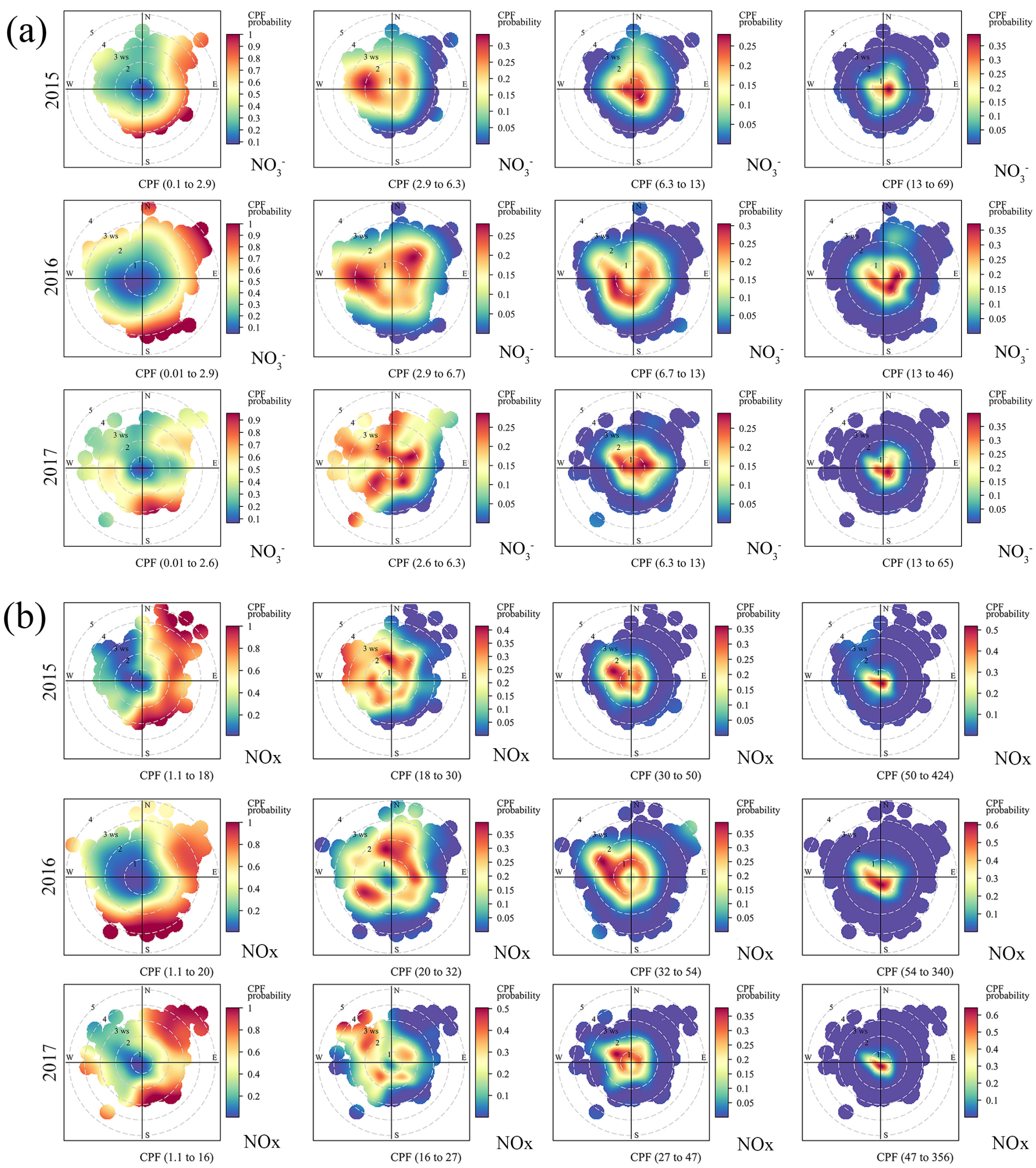

Fig. S14. PolarPlot of the NO_3^- and NOx concentrations from 2015 to 2017 in Chengdu based on the conditional probability functions (CPF) for the following ranges of percentile intervals: 0-25, 25-50, 50-75, and 75-100. (a) NO_3^-. (b) NOx.

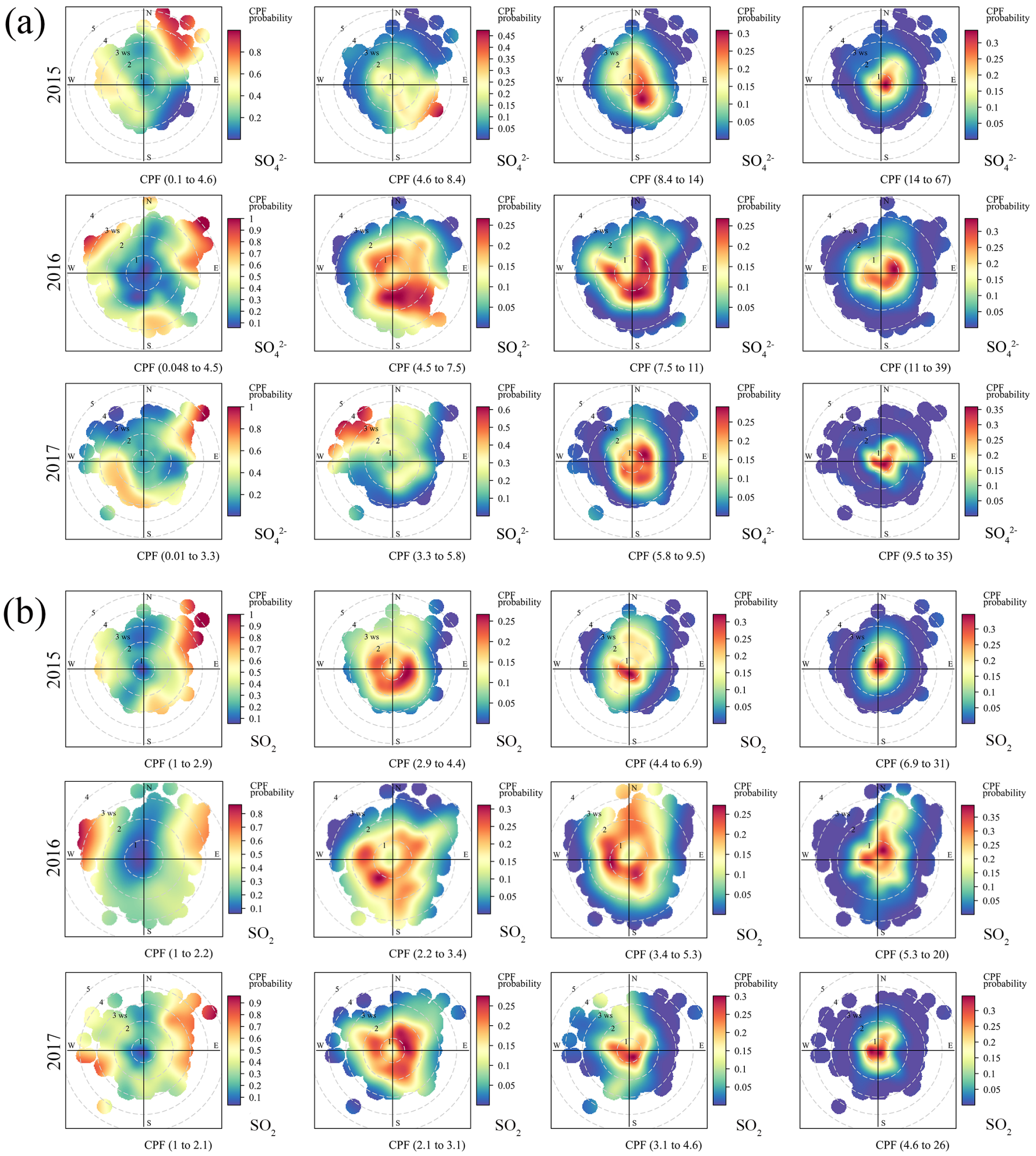

Fig. S15. PolarPlot of the SO_4^{2-} and SO_2 concentrations from 2015 to 2017 in Chengdu based on the CPF for the following ranges of percentile intervals: 0-25, 25-50, 50-75, and 75-100. (a) SO_4^{2-}. (b) SO_2.

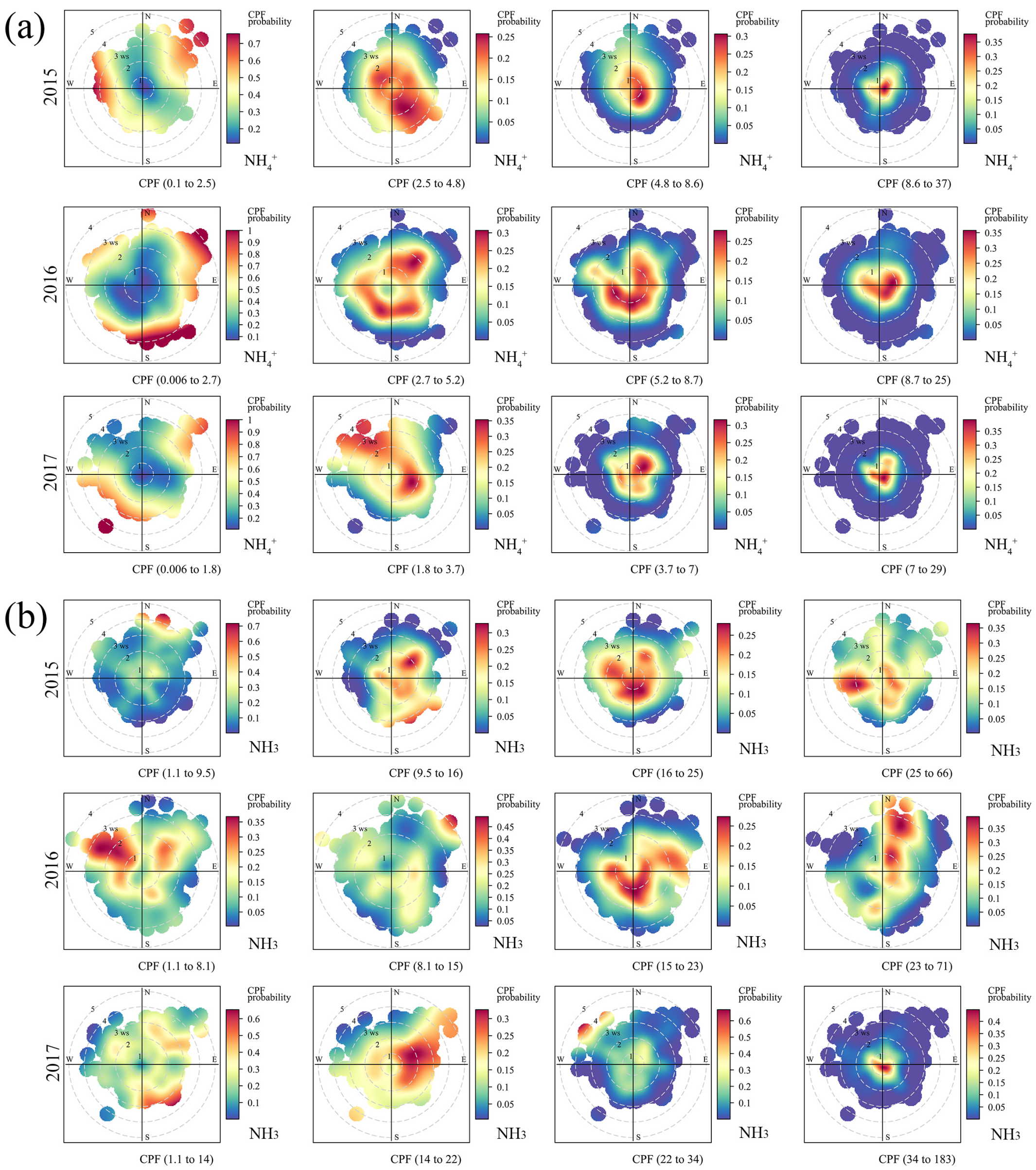

Fig. S16. PolarPlot of the NH_4^+ and NH_3 concentrations from 2015 to 2017 in Chengdu based on the CPF for the following ranges of percentile intervals: 0-25, 25-50, 50-75, and 75-100. (a) NH_4^+. (b) NH_3.

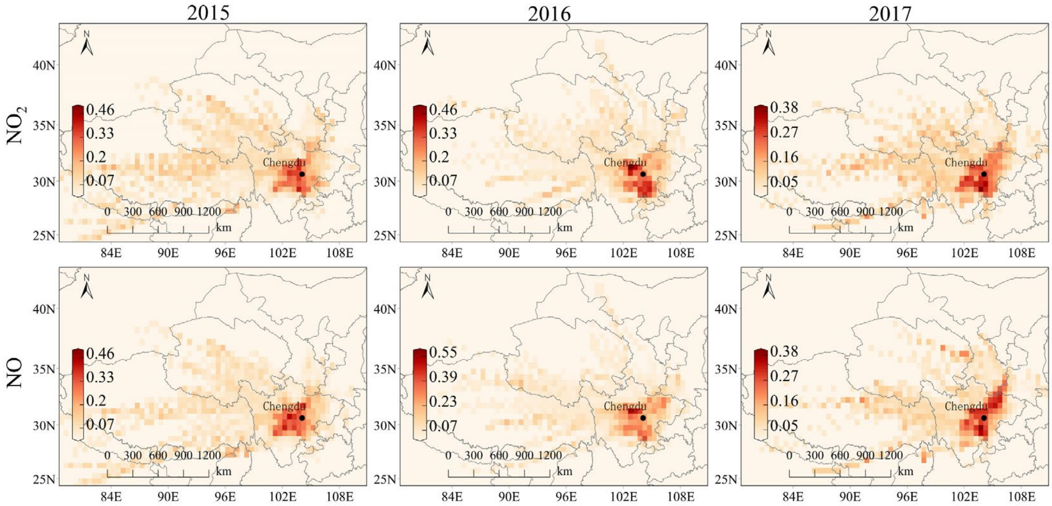

Fig. S17. PSCF (potential source contribution function) of NO_2 and NO in Chengdu from 2015 to 2017.

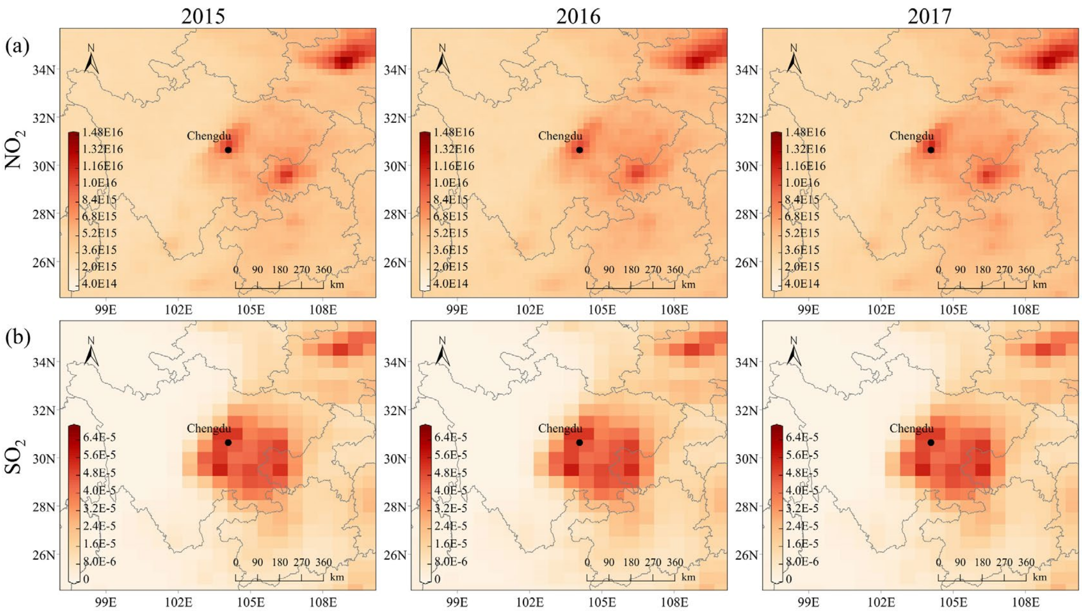

Fig. S18. Spatial distribution characteristics of NO_2 and SO_2 in the Sichuan Basin in Southwest China from 2015 to 2017. (https://giovanni.gsfc.nasa.gov/giovanni/, last access: June 17, 2020). (a) Nitrogen dioxide (NO_2) total column (30% cloud screened) ($1/cm^2$), data source: OMI. (b) Sulfur dioxide (SO_2) column mass density (kg/m^2), data source: MERRA-2 Model.

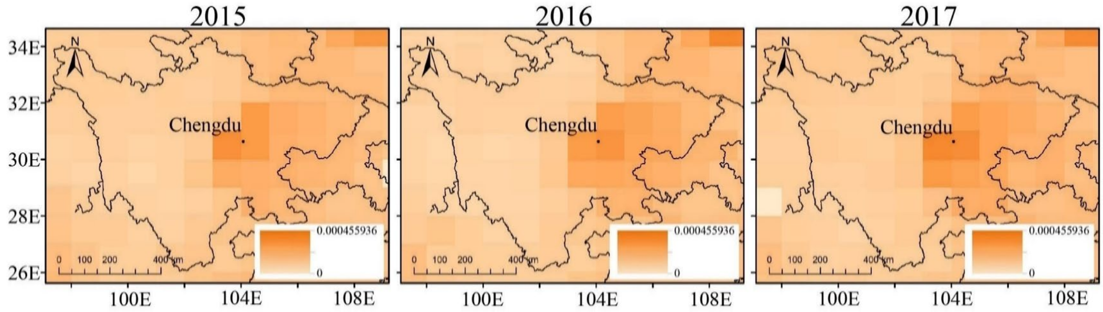

Fig. S19. NH_3 total column from IASI (Infrared Atmospheric Sounding Interferometer, https://iasi.aeris-data.fr/nh3/, last access: June 17, 2020), units: mol/m^2, grid resolution: 1°×1°, data from: Metop-B (Level 3, day data). Data processing method: Use the downloaded monthly average data from IASI to get the annual average data after processing by MeteoInfoMap and ArcMap software.

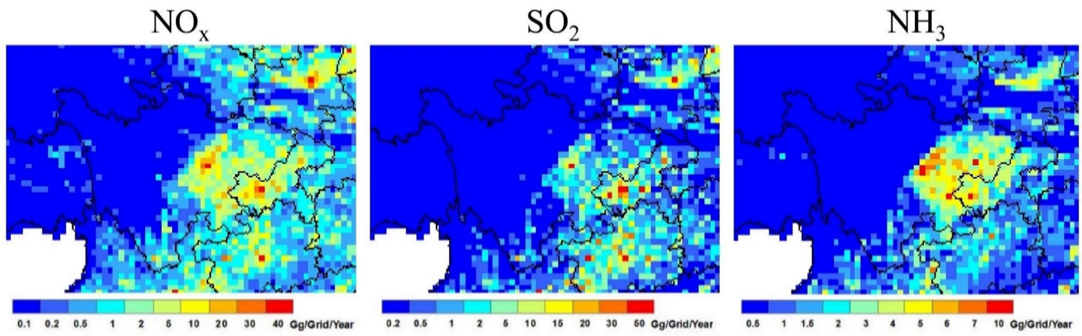

Fig. S20. Gridded NOx, SO_2 and NH_3 emissions in southwest China in 2016 from the Multiresolution Emission Inventory for China (MEIC, www.meicmodel.org, last access: June 17, 2020).

References:

Fountoukis, C., Nenes, A., Sullivan, A., Weber, R., Van Reken, T., Fischer, M., Matias, E., Moya, M., Farmer, D., and Cohen, R. C.: Thermodynamic characterization of Mexico City aerosol during MILAGRO 2006, Atmospheric Chemistry and Physics, 9, 2141-2156, https://doi.org/10.5194/acp-9-2141-2009, 2009.